

# Metal Dispersion of Bimetallic Catalysts via Stepwise Chemisorption and Surface Titration

## I. Ru-Au/SiO<sub>2</sub>

A. G. SHASTRI AND J. SCHWANK

*Department of Chemical Engineering, The University of Michigan, Ann Arbor, Michigan 48109*

Received October 3, 1984; revised March 15, 1985

A stepwise chemisorption and titration procedure involving H<sub>2</sub> and O<sub>2</sub> as adsorbates is used to measure the dispersion of the individual metal components in bimetallic Ru-Au/SiO<sub>2</sub> catalysts. The experimental approach is based upon differences in O<sub>2</sub> adsorption on Ru and Au, respectively, as a function of adsorption temperature. At room temperature, O<sub>2</sub> is adsorbed on Ru but not on Au. However, at 473 K both metals chemisorb O<sub>2</sub>, albeit with a change in adsorption stoichiometry in the case of Ru. Finally, oxygen that is adsorbed on Ru can be titrated with H<sub>2</sub> at 373 K, while oxygen that is adsorbed on Au sites does not react with H<sub>2</sub> under these conditions. The reliability of the technique is first tested on physical mixtures of Ru/SiO<sub>2</sub> and Au/SiO<sub>2</sub> of known dispersion and then applied to a series of bimetallic Ru-Au/SiO<sub>2</sub> catalysts. The results from this stepwise chemisorption procedure are critically evaluated and compared with previously obtained extensive characterization data on these catalysts. In conjunction with analytical electron microscopy and WAXS results, an estimate of the average surface composition of bimetallic particles is derived. © 1985 Academic Press, Inc.

### INTRODUCTION

Chemisorption is a widely used technique for determination of metal dispersions and average metal particle sizes in supported catalysts. For monometallic catalysts, the technique has proven to be quite reliable providing results in good agreement with electron microscopy and X-ray diffraction data. It is important to extend the applicability of gas chemisorption into the realm of bimetallic catalysts, in view of the growing academic and industrial interest in the field.

Unfortunately, the commonly used adsorbates with well-established adsorption stoichiometries tend to indiscriminately chemisorb on both metal components of a typical bimetallic catalyst. Due to limited choice of suitable adsorbates, one is often restricted to a determination of the total number of metal surface sites without gaining information about the relative distribution of the individual metal components on

the surface. A case in point is the Pt-Ir system where there is no significant difference in the chemisorption characteristics of the two metals (1).

A second complication arises in cases where the two metal components interact electronically or form alloys exhibiting an adsorption behavior that is markedly different from each of the components or their physical mixtures. Changes in adsorption strength and stoichiometry are typical symptoms. For example, different research groups proposed conflicting stoichiometries for H<sub>2</sub> and O<sub>2</sub> chemisorption and titration on Pt-Re catalysts to account for their experimental observations (1-7).

It cannot be ruled out that the composition of bimetallic particles or clusters in a given catalyst varies widely from one particle to the other resulting in variations in the adsorption parameters. Very little is known about this particular aspect, at least for bimetallic systems. However, there is evidence in monometallic catalysts for a de-

pendence of adsorption characteristics on metal dispersion.

In spite of all these difficulties, various research groups made efforts to employ chemisorption and titration techniques along with careful pretreatment to estimate metal dispersions of individual components in bimetallics. Stepwise chemisorption and titration procedures have been attempted, most notably for the Pt-Re system (6, 7), the Pt-Au system (8), and the Pt-Ru system (9). In the case of  $\text{Al}_2\text{O}_3$ -supported Pd-Ni catalysts, different reactivities of the oxidized surfaces of Ni and Pd toward hydrogen at room temperature were used in an attempt to determine the surface composition (10). The probability of success is higher in bimetallic systems such as Ru-Au where the two components have drastically different adsorption behavior and are completely immiscible in the bulk.

In recent work on supported bimetallic Ru-Au catalysts, an attempt was made to correlate the catalytic activity with the structure and morphology of these catalysts (11). A thorough and extensive characterization effort with major emphasis on analytical electron microscopy revealed that these bimetallic catalysts were quite non-uniform in terms of metal particle composition. For example, in a series of  $\text{SiO}_2$ -supported Ru-Au catalysts, a bimodal particle size distribution was found. Large metal particles ( $>15$  nm) were without exception monometallic Au, while all the Ru resided in small particles ( $<4$  nm) along with some Au. Analysis of individual small particles by X-ray energy dispersive spectroscopy (EDS) revealed that a sizable fraction of the small particles contained both metals (12). Generally, these particles contained preferentially one of the metals with only a trace of the other. The preferred composition of these particles is consistent with a bimetallic cluster model where a small amount of one metal component is "adsorbed" on the surface of the other component.

One of the intriguing questions regarding such bimetallic clusters is their surface composition. It is well known that even

small amounts of Cu or Au can lead to dramatic changes in the specific activity of Ru (13, 14). Analytical electron microscopy, as useful as it is for giving semiquantitative information about the elemental composition of bimetallic clusters, cannot provide data concerning their surface composition. The limitations of analytical electron microscopy for the characterization of such small particles are discussed elsewhere (12). To take the characterization of the Ru-Au catalysts one step further and to address the issue of the surface composition of the bimetallic clusters, a stepwise chemisorption procedure was employed with the goal to determine the dispersion of Ru and Au separately.

In the case of the Ru-Au system, we have substantial evidence from previous work that the interaction between Ru and Au is predominantly geometric and not electronic in nature (11, 14). Therefore, it could be hoped that the chemisorption behavior of the two metals would not be significantly altered by the presence of the second component. We perceived a good opportunity to succeed with such a stepwise chemisorption approach, especially since we could take advantage of the markedly different chemisorption behavior of the two metals. The stepwise chemisorption and gas titration results are interpreted in the light of the detailed structural and analytical information available from electron microscopy and X-ray diffraction. The discussion here is restricted to  $\text{SiO}_2$ -supported Ru-Au catalysts. Stepwise chemisorption on an analogous series of MgO-supported bimetallic Ru-Au catalysts is the subject of Part II (15).

#### EXPERIMENTAL

The chemisorption experiments were carried out in a static volumetric Pyrex glass high-vacuum system. Research grade gases were used for catalyst pretreatment and chemisorption. Figure 1 gives a summary of the steps involved in catalyst pretreatment and chemisorption. The dispersion of Ru was measured independently by

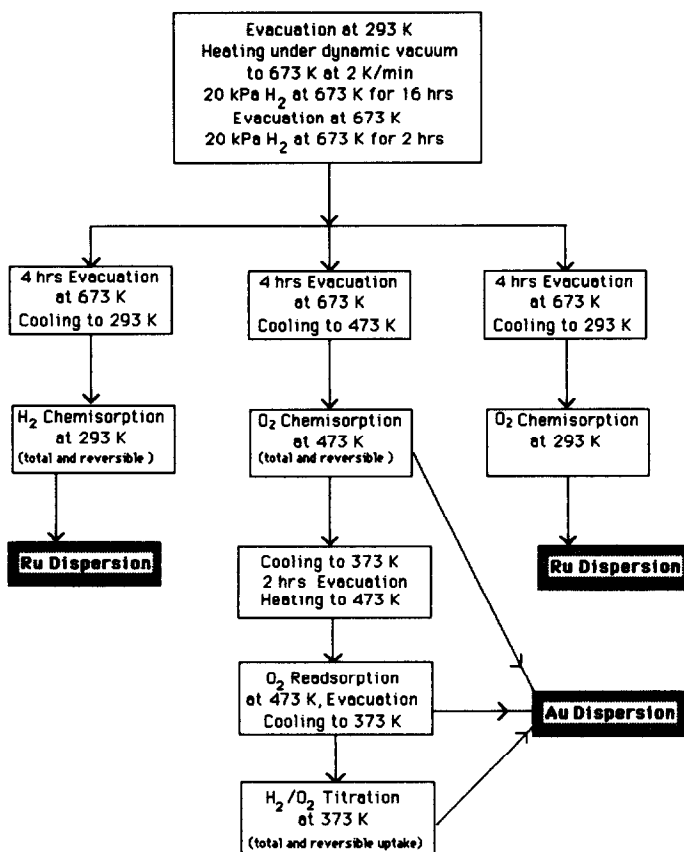


FIG. 1. Flow diagram showing the steps involved in pretreatment and chemisorption/titration experiments carried out to determine the individual metal dispersions in supported Ru–Au bimetallic catalysts.

both H<sub>2</sub> and O<sub>2</sub> chemisorption at 293 K. To gain information about the dispersion of Au, a stepwise procedure was used which included O<sub>2</sub> chemisorption at 473 K, followed by cooling to 373 K, evacuation, and H<sub>2</sub>/O<sub>2</sub> titration at 373 K. Typically, equilibration times of 1 hr were allowed for each adsorption point.

The amount of strongly bound H<sub>2</sub> was measured by taking the difference between two isotherms obtained sequentially. The first isotherm provided information about the total gas uptake. The second isotherm after 30 min evacuation gave the amount of weakly adsorbed H<sub>2</sub>. To measure the amount of strongly chemisorbed oxygen, three isotherms were obtained in the following sequence: first, the total oxygen uptake was determined at 473 K; then the

sample was evacuated at 473 K and a second adsorption isotherm, labeled "reversible," was obtained at the same temperature. Finally, the sample was cooled to 373 K and evacuated for 2 hr. During evacuation at 373 K, some oxygen in addition to the reversibly adsorbed oxygen at 473 K could be removed from ruthenium sites. Oxygen adsorbed on Au sites at 473 K could not be removed by evacuation at 473 or 373 K, as proven by experiments with monometallic Au catalysts which will be described in detail later on. Then the temperature was raised again to 473 K and a third adsorption isotherm, labeled "readsorption," was obtained. It should be noted that the oxygen uptake reported for the "readsorption" is already corrected for the amount of "reversible" oxygen uptake at

473 K. Thus, the oxygen uptake obtained in the "readsorption" isotherms is a direct measure of the amount of oxygen that could be removed from the Ru sites by evacuation at 373 K. The difference between the first adsorption isotherm and the sum of the "reversible" and "readsorption" isotherms provided the amount of strongly chemisorbed oxygen that could not be removed at temperatures of 373 to 473 K. The strongly bound oxygen on Ru sites was titrated with H<sub>2</sub> at 373 K. Oxygen associated with gold sites cannot be titrated with H<sub>2</sub> at 373 K which is of crucial importance for the determination of individual metal dispersions in our system. Since the gold dispersion is calculated from the difference between strongly adsorbed oxygen obtained from the three above-mentioned isotherms and the titratable oxygen at 373 K (which corresponds to oxygen on ruthenium sites), failure to take the weakly bound oxygen at 373 K into account would lead to erroneous results for the gold dispersion.

Monolayer adsorption volumes were obtained by extrapolating the flat portion of the adsorption isotherms to zero pressure. From these monolayer volumes, metal dispersions were derived based on assumptions concerning the adsorption stoichiometry which will be discussed under Results. Surface average metal particle sizes  $d$  were determined using the equation

$$d = 6/S\rho, \quad (1)$$

where  $S$  represents the metal surface area per gram of metal, and  $\rho$  the density of the metal. For calculating the metal surface area  $S$ , cross-sectional areas of 9.03 Å<sup>2</sup> per Ru surface atom (19) and 9.13 Å<sup>2</sup> per Au surface atom (17) were assumed.

The samples used for the chemisorption experiments were taken from a series of catalysts that were prepared by impregnation of SiO<sub>2</sub> supports with RuCl<sub>3</sub> · H<sub>2</sub>O and HAuCl<sub>4</sub> · 3H<sub>2</sub>O precursor compounds. These samples have been thoroughly characterized in previous work (11, 14, 16–18). Table 1 summarizes some of the pertinent

TABLE 1  
Characterization Data from Previous Work (14)

Code	Ru <sup>a</sup> (wt%)	Au <sup>a</sup> (wt%)	H/Ru <sup>b</sup>	O <sub>2</sub> /Ru <sup>b</sup>	WAXS <sup>c</sup>	
					Ru	Au
RS091	3.32	0.61	0.29	0.28	<4	44.8
RS048	1.66	3.47	0.23	0.28	<4	38.7
RS014	0.39	4.65	0.30	0.32	<4	23.7

<sup>a</sup> Weight percentage of metal as determined by atomic absorption.

<sup>b</sup> Ruthenium dispersion determined by chemisorption at room temperature.

<sup>c</sup> Average metal particle size in nanometers as obtained from WAXS line broadening. Ru particle size is reported as <4 nm since no Ru peak could be detected by WAXS. For Au, the (220) peak was used.

characterization data. In addition to the bimetallic Ru–Au/SiO<sub>2</sub> catalysts, two physical mixtures of monometallic Ru/SiO<sub>2</sub> and Au/SiO<sub>2</sub> were made by combining varying amounts of the two catalysts. One of these physical mixtures (code name RSP055) contained 55 at.% Ru, the other (code name RSP017) had 17 at.% Ru. The monometallic samples and their physical mixtures were characterized according to all the steps outlined in Fig. 1. Identical pretreatment and experimental conditions were also used to check the gas uptake on the blank supports.

## RESULTS AND DISCUSSION

In order to extract meaningful results for bimetallic Ru–Au catalysts from the stepwise chemisorption and titration procedure outlined under Experimental, it is necessary to understand first how the individual metal components and the blank support behave under the experimental conditions. Then, the stepwise chemisorption technique can be tested on physical mixtures of the two monometallic catalysts Ru/SiO<sub>2</sub> and Au/SiO<sub>2</sub>. Assuming that there are no interactions between Ru and Au in these physical mixtures, the approach is as follows: first, the dispersion of Ru alone is determined via H<sub>2</sub> chemisorption at room temperature. Au does not adsorb H<sub>2</sub> under these conditions. Then, O<sub>2</sub> is adsorbed both on Ru and Au sites at 473 K. After lowering

the temperature to 373 K and evacuation (which removes some of the adsorbed oxygen from Ru sites, but not from Au) oxygen that is adsorbed on Ru sites is titrated with H<sub>2</sub>. Oxygen held on Au sites cannot be titrated with H<sub>2</sub> at 373 K. From the amount of H<sub>2</sub> consumed in the titration, it is possible to determine the oxygen that was adsorbed on Ru. Thus, we should be in a position to determine the Ru and Au dispersion in the physical mixtures separately and compare the results with the known metal dispersion values of the monometallic catalysts. Finally, the technique is used on bimetallic Ru–Au/SiO<sub>2</sub> catalysts and the results are used in conjunction with WAXS and electron microscopy data to arrive at an estimate of the average surface composition of the bimetallic particles in the catalysts. Experiments carried out on the blank SiO<sub>2</sub> support that had been subjected to the standard pretreatment showed no uptake of H<sub>2</sub> and O<sub>2</sub> in the temperature range from 293 to 573 K.

#### Chemisorption on Ru/SiO<sub>2</sub>

To investigate the behavior of Ru in the stepwise chemisorption procedure, experiments were carried out first on a monometallic Ru/SiO<sub>2</sub> catalyst with the code name S-1-673. This catalyst had a loading of 3 wt% Ru and was prepared by impregnation of SiO<sub>2</sub> with an aqueous solution of RuCl<sub>3</sub> · H<sub>2</sub>O. On this catalyst, a considerable amount of reversible H<sub>2</sub> adsorption was found at 293 K. The reversible portion of hydrogen adsorption was almost negligible at low pressures, but became very significant at higher pressures (Fig. 2). Reversible adsorption of hydrogen on Ru has been reported previously (19–22). For irreversibly chemisorbed hydrogen, H/Ru<sub>s</sub> stoichiometries of approximately 1/1 were generally found (19–28). Based on this stoichiometry, the irreversible H<sub>2</sub> uptake on catalyst S-1-673 would correspond to a Ru dispersion of 39.1% or an average Ru particle size of 2.3 nm (Table 2). The O<sub>2</sub> uptake on the Ru/SiO<sub>2</sub> catalyst S-1-673 at 293 K was ap-

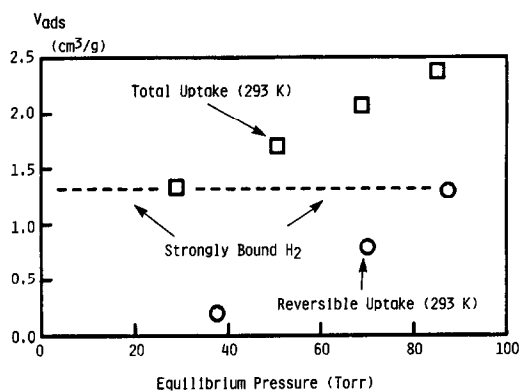


FIG. 2. H<sub>2</sub> chemisorption on Ru/SiO<sub>2</sub> (S-1-673) at 293 K. The amount of strongly bound H<sub>2</sub> (---) is obtained by subtracting the reversible uptake (○) from the total uptake (□).

proximately twice as large as the uptake of H<sub>2</sub> (Table 2), a phenomenon already previously observed on other Ru/SiO<sub>2</sub> catalysts (14, 18). This indicates a stoichiometry of Ru<sub>s</sub>O<sub>2</sub>, in agreement with the surface oxide stoichiometry proposed by Kubicka (20). While room-temperature adsorption seemed to lead to surface oxide formation, a much higher uptake of O<sub>2</sub> was obtained when the chemisorption was carried out at 473 K (Fig. 3, Table 2). It has to be noted that it is necessary to study the behavior of Ru at this adsorption temperature since this temperature will be required later in the bimetallics to achieve oxygen adsorption on Au. The increased uptake of O<sub>2</sub> on Ru/SiO<sub>2</sub> at 473 K could be due to several reasons, namely oxygen spillover, or formation of surface oxides such as Ru<sub>s</sub>O<sub>3</sub> and Ru<sub>s</sub>O<sub>4</sub>, or formation of subsurface and bulk ruthenium oxide.

To check the first possibility, namely oxygen spillover onto the support, experiments were carried out on unsupported Ru metal that was obtained by reduction of RuO<sub>2</sub> powder in H<sub>2</sub> at 673 K for 16 hr. At 293 K, the Ru metal showed an oxygen uptake of 0.24 cm<sup>3</sup>(STP)/g, while at 473 K the oxygen uptake increased to 2.64 cm<sup>3</sup>(STP)/g. This result convincingly proves that oxygen at higher temperatures can interact with subsurface atoms of Ru. Furthermore,

TABLE 2

Gas Uptake, Percentage Metal Dispersion, and Particle Sizes for Monometallic Catalysts and Their Physical Mixtures

Sample (wt%) (Code)	H <sub>2</sub> (293 K)			O <sub>2</sub> (293 K)			O <sub>2</sub> (473 K)			H <sub>2</sub> /O <sub>2</sub> (373 K)		
	cm <sup>3</sup> /g	%D (Ru)	<i>d</i> (nm)	cm <sup>3</sup> /g	%D (Ru)	<i>d</i> (nm)	cm <sup>3</sup> /g	%D (Au)	<i>d</i> (nm)	cm <sup>3</sup> /g	%D (Au)	<i>d</i> (nm)
Ru/SiO <sub>2</sub> (3 wt% Ru) (S-1-673)	1.3	39.1	2.3	2.55	38.3	2.4	5.21	—	—	11.3	—	—
Au/SiO <sub>2</sub> (2.21 wt% Au) (AS4433)	—	—	—	—	—	—	0.077	12.7	9.1	—	—	—
Ru + Au/SiO <sub>2</sub> (0.94 wt% Ru) (1.52 wt% Au) (RSP055)	—	—	—	0.80	38.4	2.4	1.62	—	—	3.4	12.3	9.0
Ru + Au/SiO <sub>2</sub> (0.21 wt% Ru) (2.06 wt% Au) (RSP017)	—	—	—	0.18	38.5	2.4	0.39	—	—	0.69	12.3	9.0

the large oxygen affinity of Ru together with the inability of the blank SiO<sub>2</sub> support to chemisorb oxygen under the experimental conditions rules out oxygen spillover onto SiO<sub>2</sub> as a reason for the increased oxygen uptake on Ru/SiO<sub>2</sub> at 473 K.

As a second explanation for increased oxygen uptake on Ru at 473 K, the formation of surface oxides such as Ru<sub>5</sub>O<sub>3</sub> or Ru<sub>5</sub>O<sub>4</sub> could be envisioned. When RuO<sub>2</sub> is heated in presence of oxygen, RuO<sub>3</sub> is formed as the predominant gas phase species at temperatures higher than 1273 K, while at about 1073 K, RuO<sub>4</sub> is formed (31, 32). Therefore, it cannot be excluded that such Ru<sub>5</sub>O<sub>x</sub> species exist on the surface of Ru when it is exposed to oxygen at very high temperatures. In an XPS study of the Ru–oxygen system, a surface layer of Ru<sub>5</sub>O<sub>3</sub> was found to be present in the form of a gross defect structure of RuO<sub>2</sub> (33). A study of O<sub>2</sub> adsorption on RuO<sub>2</sub> (34) indicated that Ru<sub>5</sub>O<sub>x</sub> species can form on the surface of RuO<sub>2</sub>, where the value of *x* depends on the temperature and O<sub>2</sub> partial pressure. Our oxygen adsorption experiments were carried out at temperatures well below the regime where these surface oxides would form. Furthermore, if significant amounts of Ru<sub>5</sub>O<sub>x</sub> were involved, we should have encountered severe problems with the experimental reproducibility due to the well-known instability and volatility

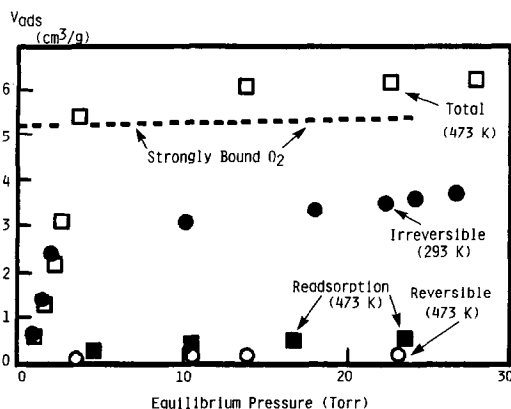
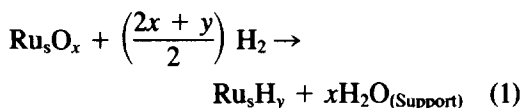


FIG. 3. O<sub>2</sub> chemisorption on Ru/SiO<sub>2</sub> (S-1-673) at different temperatures. (●) Irreversibly adsorbed O<sub>2</sub> at 293 K; (□) total uptake of O<sub>2</sub> at 473 K; (○) reversible uptake of O<sub>2</sub> at 473 K observed after evacuation at 473 K; (■) readsorption of O<sub>2</sub> at 473 K observed after cooling and evacuation at 373 K; (---) strongly bound O<sub>2</sub> at 473 K which could not be pumped off between 373 and 473 K.

of these species. In our experiments, the perfectly reproducible O<sub>2</sub> uptake in several reduction/oxidation cycles is a strong argument against the presence of Ru<sub>s</sub>O<sub>x</sub> species. If, for arguments sake, such Ru<sub>s</sub>O<sub>x</sub> surface species were present, the titration with H<sub>2</sub> would take place according to the following reaction stoichiometry:

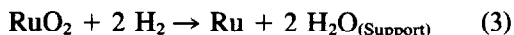


If one assumes that  $x = 4$  and  $y = 1$ , a H<sub>2</sub> uptake of approximately 11.7 cm<sup>3</sup>(STP)/g would be required, compared to the experimental result of 11.3 cm<sup>3</sup>(STP)/g (see Fig. 4).

Finally, the increased oxygen uptake on Ru/SiO<sub>2</sub> at 473 K could be due to the formation of subsurface and bulk RuO<sub>2</sub>. On Ru black, it has been observed that the oxygen uptake increased beyond monolayer coverage with increasing temperature; this phenomenon was ascribed to the penetration of oxygen into the bulk of the Ru metal (29). The extent of diffusion of oxygen into the bulk of Ru leading to the formation of RuO<sub>2</sub> depends on temperature, particle size, and equilibration time. In previous isotopic oxygen exchange experiments on Ru/SiO<sub>2</sub> that had been equilibrated in oxygen at 573 K, it was found that not just the Ru surface,

but also subsurface layers of Ru were involved in oxygen exchange (30). The exchangeable solid-phase oxygen was associated with Ru, probably in form of RuO<sub>2</sub>. However, the kinetics of the isotopic oxygen exchange reaction on Ru/SiO<sub>2</sub> indicated the presence of nonuniformities in oxygen bond strength and/or the onset of diffusional limitations after a certain degree of isotopic oxygen exchange. Complete oxidation of all the Ru to RuO<sub>2</sub> in our sample S-1-673 would require an O<sub>2</sub> uptake of 6.65 cm<sup>3</sup>(STP)/g which is significantly higher than the experimentally observed uptake of 5.21 cm<sup>3</sup>(STP)/g (Table 2). This latter number represents the volume of strongly bound oxygen that could not be removed by evacuation in the temperature range of 373 to 473 K (Fig. 3). The fact that the O<sub>2</sub> uptake was less than theoretically expected for complete oxidation of all the Ru indicates that the formation of RuO<sub>2</sub> does not go to completion under our reaction conditions and involves only about 80% of the total Ru in the sample. This is in agreement with the observed nonuniformities in the oxygen exchange on Ru/SiO<sub>2</sub> (30).

In the event of bulk oxide formation, the following two reactions would take place during H<sub>2</sub>/O<sub>2</sub> titration (Fig. 4):



Reaction (2) would take place on Ru surface atoms, while reaction (3) would involve Ru atoms in the subsurface and the bulk region of the particles. The probability for the occurrence of either one of these two reactions can be assumed to be proportional to the fraction of surface and bulk Ru atoms, respectively. On collision of an oxygen gas molecule with a Ru surface site, the probability of further interaction of the adsorbed oxygen with subsurface Ru atoms seems to be comparable to the probability of surface diffusion to a vacant Ru surface site (30). From the experimentally observed H<sub>2</sub> uptake of 11.3 cm<sup>3</sup>(STP)/g in the

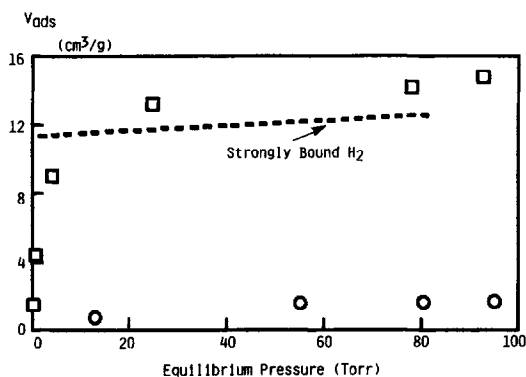


FIG. 4. H<sub>2</sub>–O<sub>2</sub> titration on Ru/SiO<sub>2</sub> (S-1-673) at 373 K. (—) Strongly bound H<sub>2</sub> obtained by graphically subtracting the reversible uptake (○) from the total uptake (□) of hydrogen.

H<sub>2</sub>/O<sub>2</sub> titration (Fig. 4, Table 2), one can calculate the amount of oxygen on Ru as

$$V_{O_2, Ru} = \frac{V_{H_2, t}}{2.5} \cdot D + \frac{V_{H_2, t}}{2} \cdot (1 - D) \quad (4)$$

$V_{O_2, Ru}$  represents the volume (cm<sup>3</sup>(STP)/g) of strongly held oxygen at 473 K, while  $V_{H_2, t}$  represents the volume (cm<sup>3</sup>(STP)/g) of H<sub>2</sub> needed in the H<sub>2</sub>/O<sub>2</sub> titration at 373 K.  $D$  is the fractional dispersion of Ru as determined by H<sub>2</sub> chemisorption at 293 K. Using Eq. (4) and 11.3 cm<sup>3</sup>(STP)/g for  $V_{H_2, t}$ , one obtains a theoretical value of 5.208 cm<sup>3</sup>(STP)/g for  $V_{O_2, Ru}$ . This number is in excellent agreement with the experimentally observed O<sub>2</sub> uptake of 5.21 cm<sup>3</sup>(STP)/g on catalyst S-1-673 at 473 K (see Table 2). The H<sub>2</sub>/O<sub>2</sub> titration results support the hypothesis that oxygen at 473 K interacts not only with the surface but also the subsurface atoms of Ru, forming mainly RuO<sub>2</sub>. However, the results obtained in the H<sub>2</sub>/O<sub>2</sub> titration do not allow one to unambiguously differentiate between the bulk oxide model versus the surface-stabilized Ru<sub>s</sub>O<sub>x</sub> model. Fortunately, for our purpose it is not crucial to know which model best describes the interaction of Ru with O<sub>2</sub>. For the dispersion measurement on the bimetallics via the stepwise chemisorption and titration procedure, it is only important to know the relative amount of oxygen held on Ru which can be titrated with H<sub>2</sub> at 373 K.

#### *Chemisorption on Au/SiO<sub>2</sub>*

It is generally accepted that Au cannot chemisorb H<sub>2</sub> and O<sub>2</sub> at room temperature. Experimental observations made in our laboratories are in agreement. Even at elevated temperatures, Au is not able to chemisorb detectable amounts of molecular H<sub>2</sub>. The inability of Au to dissociate H<sub>2</sub> is well documented. Chemisorption of oxygen on Au at elevated temperatures is still not fully understood and conflicting reports can be found. A recent literature survey on the catalytic properties on Au has addressed questions of gas chemisorption on Au in more detail (35). It has been found that sup-

ported Au catalysts can chemisorb oxygen at 473 K; Au dispersion values and particle sizes in good agreement with X-ray diffraction and electron microscopy results could be obtained by assuming a Au<sub>s</sub>/O<sub>2</sub> stoichiometry of 4 (36–38).

A monometallic Au/SiO<sub>2</sub> catalyst with code name A-4433, containing 2.21 wt% Au and prepared by impregnation of SiO<sub>2</sub> support with an aqueous solution of HAuCl<sub>4</sub> · 3H<sub>2</sub>O was used for chemisorption. Oxygen was found to strongly adsorb at 473 K (Table 2) and could not be removed from the gold sites by evacuation at 473 and 373 K. Moreover, in contrast to ruthenium, the oxygen that was chemisorbed on gold could not be removed by titration with H<sub>2</sub> at 373 K, probably due to the inability of gold to generate atomic hydrogen. No consumption of H<sub>2</sub> was found at 373 K at H<sub>2</sub> partial pressures up to 50 Torr (1 Torr = 133.3 N m<sup>-2</sup>). However, the adsorbed oxygen could be completely removed from the Au surface by evacuation at 293 K. This observation is in agreement with the adsorption isobar of oxygen on Au showing a maximum at about 473 K and a minimum at room temperature (36).

#### *Chemisorption on Physical Mixtures of Ru/SiO<sub>2</sub> and Au/SiO<sub>2</sub>*

In order to test the reliability of the stepwise chemisorption for bimetallics, the technique was first applied to physical mixtures of the Ru/SiO<sub>2</sub> catalyst S-1-673 and the Au/SiO<sub>2</sub> catalyst A-4433. The objective was to see whether the Ru and Au dispersion values obtained by applying the stepwise chemisorption procedure were in agreement with the already known values for the monometallic samples. Table 2, which shows the amount of strongly chemisorbed gases indicates that the results from the stepwise chemisorption procedure are in excellent agreement with the known values for the monometallic samples. Figure 5 shows the oxygen adsorption isotherms on one of the physical mixtures (RSP055). Figure 6 gives the results for the H<sub>2</sub>/O<sub>2</sub> titra-



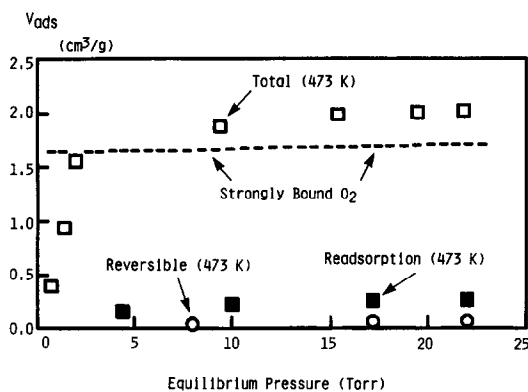


FIG. 5. O<sub>2</sub> chemisorption on physical mixture RSP055 at 473 K. (□) Total uptake at 473 K; (○) reversible uptake at 473 K observed after evacuation at 473 K; (■) readsorption of O<sub>2</sub> at 473 K after cooling and evacuation at 373 K; (---) strongly bound O<sub>2</sub> obtained by subtracting the reversible (○) and readsorbed O<sub>2</sub> (■) from the total O<sub>2</sub> uptake at 473 K (□).

tion. From the strongly bound oxygen at 473 K (Fig. 5), and the strongly bound H<sub>2</sub> in the titration at 373 K (Fig. 6), the oxygen held on Ru sites can be differentiated from the oxygen held on Au sites (see Fig. 1).

#### Chemisorption on Bimetallics

For the Ru–Au/SiO<sub>2</sub> catalysts, information about the particle size distribution and relative allocation of the two metals to a given particle size range is already available through an extensive characterization by analytical electron microscopy. The details of the microscopy work are published elsewhere (11, 12). A brief summary of the microscopy results is given below in order to allow a correlation with the chemisorption data. Transmission electron microscopy showed a clear bimodal metal particle size distribution in all three bimetallic samples. Numerous very small particles in the size range of 1–4 nm were found, along with a few large particles (>15 nm). There was a complete absence of particles of intermediate size (4–15 nm). Elemental analysis of these particles by X-ray energy dispersive spectroscopy (EDS) showed that all the large particles, without exception, were monometallic Au particles. All the Ru in

these catalysts was contained in the small particles (<4 nm). Individual analysis of these small particles proved that the composition of the particles was nonuniform. The analytical microscopy data do not allow accurate quantification of the two metals due to the weak X-ray signals generated in such small metal particles and the resulting poor peak to background ratios in the EDS spectra. Therefore, the EDS data can only be used for qualitative estimates of particle compositions. On the basis of the EDS results, a model was proposed for the structure of the small bimetallic particles where one metal component is “adsorbed” on the surface of the other (11, 12). This “adsorption” model is corroborated by the results obtained in ethane hydrogenolysis (14) and CO hydrogenation (11, 39). The specific activity of Ru dropped by orders of magnitude as a function of Au content, and this phenomenon was explained on the basis of a geometric dilution effect of active Ru surface ensembles by inactive Au. Further support for the geometric and not electronic nature of the Ru–Au interaction comes from infrared spectroscopy. The spectra of CO adsorbed on the Ru–Au/SiO<sub>2</sub> catalysts showed no significant shifts in CO band position compared to that observed on monometallic Ru/SiO<sub>2</sub> (12). All this evidence pointing toward a geometric rather

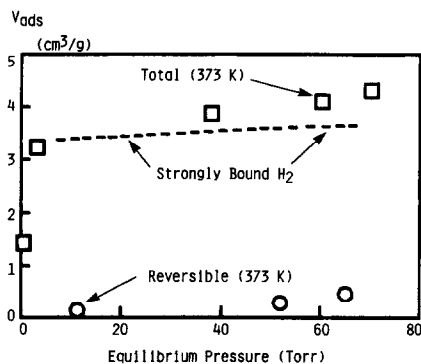


FIG. 6. H<sub>2</sub>–O<sub>2</sub> titration at 373 K on the physical mixture RSP055. The strongly bound H<sub>2</sub> (---) is obtained by graphical subtraction of the reversible H<sub>2</sub> uptake (○) from the total H<sub>2</sub> uptake (□).

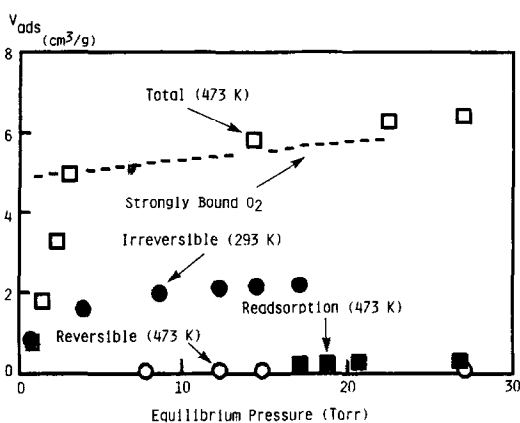


FIG. 7.  $O_2$  chemisorption on the bimetallic catalyst RS091 at different temperatures. (●) Irreversible uptake at 293 K; (□) total uptake at 473 K; (○) reversible uptake at 473 observed after evacuation at 473 K; (■) readsorption of  $O_2$  at 473 K after evacuation at 373 K; (---) strongly bound  $O_2$  obtained by graphical subtraction of reversible (○) and readsorbed  $O_2$  (■) from total uptake (□).

than electronic interaction between the two metals suggests that there is probably no significant modification of the chemisorption behavior of Ru and Au in these bimetallic catalysts, especially since the probe molecules ( $H_2$  and  $O_2$ ) are small and not sensitive to ensemble effects. Therefore, it is justified to interpret the chemisorption data on the bimetallic samples by using the same approach as applied to the physical mixtures.

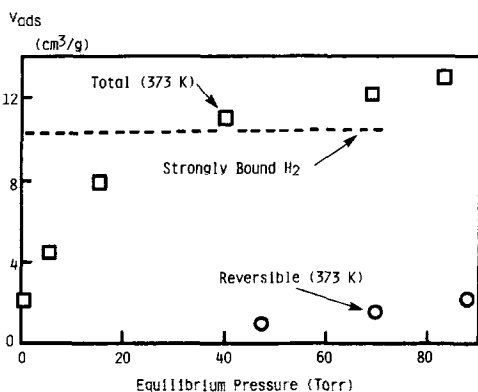


FIG. 8.  $H_2$ - $O_2$  titration on the bimetallic catalyst RS091 at 373 K. (---) Strongly bound  $H_2$  at 373 K obtained by graphical subtraction of reversible  $H_2$  uptake (○) from total  $H_2$  uptake (□).

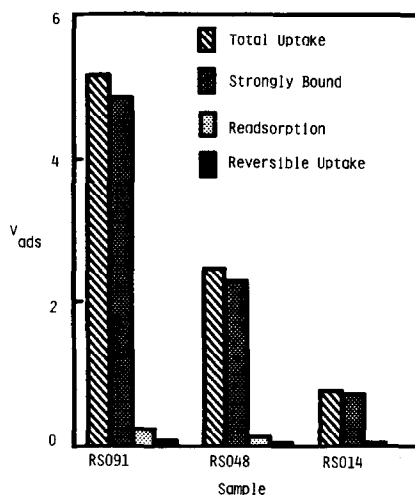


FIG. 9. Bar graphs summarizing the uptake of oxygen at 473 K on the bimetallic catalysts RS091, RS048, and RS014. The adsorbed volume ( $V_{ADS}$ ) is given in  $cm^3(STP)/g$  of catalyst.

Figures 7 and 8 show the results of oxygen chemisorption and  $H_2/O_2$  titration on catalyst RS091. A summary for the data obtained on all three bimetallic catalysts is given in the form of bar graphs in Figs. 9 and 10. Table 3 presents dispersion and particle size results for Ru and Au. In a strict

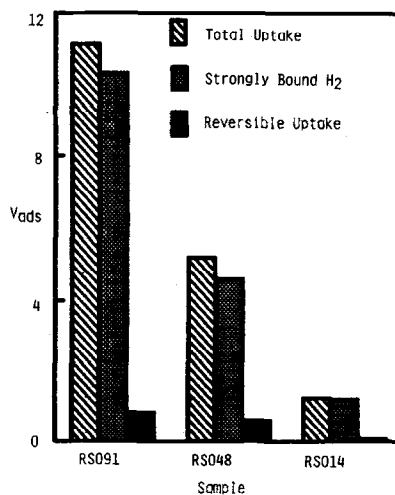


FIG. 10. Bar graphs summarizing the uptake of hydrogen during  $H_2$ - $O_2$  titration at 373 K on the bimetallic catalysts RS091, RS048, and RS014. The adsorbed volume ( $V_{ADS}$ ) is given in  $cm^3(STP)/g$  of catalyst.

TABLE 3  
Gas Uptake, Percentage Metal Dispersion, and Particle Sizes for Bimetallic Catalysts

Sample (wt%) (Code)	H <sub>2</sub> (293 K)			O <sub>2</sub> (293 K)			O <sub>2</sub> (473 K) (cm <sup>3</sup> /g)	H <sub>2</sub> /O <sub>2</sub> (373 K)		
	cm <sup>3</sup> /g	%D (Ru)	<i>d</i> (nm)	cm <sup>3</sup> /g	%D (Ru)	<i>d</i> (nm)		cm <sup>3</sup> /g	%D (Au)	<i>d</i> (nm)
RuAu/SiO <sub>2</sub> (3.32 wt% Ru) (0.61 wt% Au) (RS091)	1.08	29.3	3.3	1.8	24.5	3.5	4.867	10.3	9.1	12.3
RuAu/SiO <sub>2</sub> (1.66 wt% Ru) (3.47 wt% Au) (RS048)	0.42	23.0	3.6	0.825	22.4	3.6	2.275	4.6	8.2	13.6
RuAu/SiO <sub>2</sub> (0.39 wt% Ru) (4.65 wt% Au) (RS014)	0.13	30.0	2.9	0.295	34.1	2.7	0.736	1.17	13.7	8.1

sense, only Au and Ru dispersions can be directly measured by the stepwise chemisorption procedure. However, when combined with WAXS and electron microscopy results, an approximate estimation of the average surface composition of the bimetallic particles can be attempted. For this purpose, it is assumed that the average gold particle size derived from WAXS accounts for Au present in form of large particles (>15 nm) only and does not include any of the Au located in small particles (<4 nm). The average Au particle sizes obtained from chemisorption (Table 3) are consistently lower than the WAXS particle sizes for Au reported in Table 1. This discrepancy clearly indicates that a certain fraction of Au must be located in the small particles (<4 nm). It is reasonable to assume that the fraction of Au that is not accounted for by WAXS is associated with Ru in the form of small bimetallic particles.

From the WAXS average particle size  $d_{w,Au}$  for the large Au particles, the Au surface area per gram of catalyst,  $S_{w,Au}$ , is calculated. Then, the total surface area per gram of catalyst,  $S_{t,Au}$ , is determined based on the results from the stepwise chemisorption procedure assuming that the latter technique accounts for all the surface Au atoms, irrespective of whether they are located in large monometallic Au particles or

in small bimetallic clusters. The difference between the chemisorption Au surface area  $S_{t,Au}$  and the WAXS Au surface area  $S_{w,Au}$  gives the Au surface area  $S_{b,Au}$  per gram of catalyst which is contributed by small bimetallic Au particles. The number of Au surface atoms in small bimetallic clusters,  $N_{sb,Au}$ , can be calculated using the equation

$$N_{sb,Au} = \frac{S_{b,Au}}{S_{t,Au}} (N_{s,Au}), \quad (5)$$

where  $N_{s,Au}$  represents the total number of Au surface atoms per gram of catalyst as obtained by the stepwise chemisorption procedure. As all the Ru in the bimetallic catalysts is located in small particles, we can obtain the number of Ru surface atoms  $N_{s,Ru}$  from H<sub>2</sub> chemisorption at 293 K. A summary of the results is shown in Table 4. The average surface compositions for the bimetallics are based on the assumption that all small particles are bimetallics containing one component adsorbed on the surface of the other. It appears that the small particles in catalysts RS091 and RS048 are ruthenium-rich, while those in catalyst RS014 are gold-rich. These findings are in good qualitative agreement with the EDS results giving predominantly Ru signals with traces of Au for the first two samples, and strong Au signals with traces of Ru for

TABLE 4  
Estimation of Surface Composition of Bimetallic Particles

Catalyst	$N_{s,Ru}$ (atoms/g)	$N_{s,Au}$ (atoms/g)	$S_{L,Au}$ (m <sup>2</sup> /g)	$S_{b,Au}$ (m <sup>2</sup> /g)	$N_{sb,Au}$ (atoms/g)	Bimetallics surface composition (at.% Ru)
RS091	$5.8 \times 10^{19}$	$1.69 \times 10^{18}$	0.154	0.087	$9.55 \times 10^{17}$	98.4
RS048	$2.26 \times 10^{19}$	$8.68 \times 10^{18}$	0.79	0.51	$5.6 \times 10^{18}$	80.1
RS014	$6.98 \times 10^{18}$	$1.95 \times 10^{19}$	1.78	1.17	$1.28 \times 10^{19}$	35.0

RS014. The increasing concentration of inactive Au on the surface of the bimetallic particles as a function of bulk Au content supports the hypothesis of a geometric dilution effect invoked in earlier kinetic studies to explain the precipitous drop in catalytic activity (14, 39). It is to be noted that in the Ru–Au/SiO<sub>2</sub> catalysts the burden of catalytic activity is carried by Ru surface sites located in particles in the small-size range (<4 nm) while all the larger particles are without exception monometallic Au which does not participate in the catalytic action.

#### CONCLUSIONS

A stepwise chemisorption and titration procedure was successfully employed to determine the dispersion of individual metal components in bimetallic Ru–Au/SiO<sub>2</sub> catalysts. The reliability of the technique was tested using physical mixtures of already characterized monometallic Ru/SiO<sub>2</sub> and Au/SiO<sub>2</sub> catalysts. Then, a series of bimetallic Ru–Au/SiO<sub>2</sub> catalysts was subjected to the same procedure. The results obtained proved the existence of small (<4 nm) bimetallic particles in these catalysts, in excellent agreement with previously obtained analytical electron microscopy data.

This study has demonstrated that oxygen chemisorption and H<sub>2</sub>/O<sub>2</sub> titration can provide reasonable estimates of individual metal dispersions in bimetallic catalysts provided there is a significant difference in

chemisorption behavior of the two metal components. A suitable choice of adsorbates and temperature regimes for chemisorption can be used to exploit these differences. Both the weakly and strongly adsorbed gas volumes have to be determined. Calculations for dispersions or surface compositions proved to be more reliable when based on the strongly adsorbed gas uptake. To derive meaningful information it is, however, necessary to ascertain that the chemisorption characteristics of one metal are not significantly altered by the presence of the other metal. This prerequisite is readily met by the Ru–Au system containing components which are immiscible in the bulk state.

Estimates of surface compositions can be made in conjunction with detailed analytical electron microscopy and WAXS data. These surface composition values represent an overall average and do not necessarily imply that the majority of bimetallic particles have the indicated surface compositions.

#### ACKNOWLEDGMENTS

Financial support for this research by the National Science Foundation through Grant CPE 8212473 is gratefully acknowledged. The authors would also like to thank Dr. S. Galvagno, Dr. G. R. Tauszik, Dr. A. K. Datye, and Mr. Jim Lee for their contributions to the work on the Ru–Au system.

#### REFERENCES

1. Charcosset, H., *Int. Chem. Eng.* **23**, 187 (1983).

2. Menon, P. G., Sieders, J., Streefkerk, F. J., and Van Keulen, G. J., *J. Catal.* **29**, 188 (1973).
3. Menon, P. G., and Prasad, J., in "Proceedings, 6th International Congress on Catalysis, London, 1976" (G. C. Bond, P. B. Wells, and F. C. Tompkins, Eds.), p. 1061. The Chemical Society, London, 1976.
4. Bolivar, C., Charcosset, H., Frèty, R., Primet, M., Tournayan, L., Betizeau, C., Leclercq, G., and Maurel, R., *J. Catal.* **45**, 163 (1976).
5. Charcosset, H., Frèty, R., Leclercq, G., Mendès, E., Primet, M., and Tournayan, L., *J. Catal.* **56**, 468 (1979).
6. Isaacs, B. H., and Petersen, E. E., *J. Catal.* **85**, 1 (1984).
7. Isaacs, B. H., and Petersen, E. E., *J. Catal.* **85**, 8 (1984).
8. Galvagno, S., and Parravano, G., *J. Catal.* **57**, 272 (1979).
9. Blanchard, G., Charcosset, H., Guenin, M., and Tournayan, L., *Surf. Sci.* **106**, 509 (1981).
10. Paryjczak, T., Farbotko, J. M., and Góralski, J., *J. Catal.* **88**, 228 (1984).
11. Datye, A. K., and Schwank, J., in "Proceedings, 8th International Congress on Catalysis, Berlin," Vol. IV, p. 587. Verlag Chemie, Weinheim, 1984.
12. Datye, A. K., Ph.D. thesis. The University of Michigan, 1984.
13. Sinfelt, J. H., *J. Catal.* **29**, 308 (1973).
14. Galvagno, S., Schwank, J., Parravano, G., Garbassi, F., Marzi, A., and Tauszik, G. R., *J. Catal.* **69**, 283 (1981).
15. Shastri, A. G., and Schwank, J., *J. Catal.* **95**, 284 (1985).
16. Schwank, J., Parravano, G., and Gruber, H. L., *J. Catal.* **61**, 19 (1980).
17. Bassi, I. W., Garbassi, F., Vlaic, G., Marzi, A., Tauszik, G. R., Cocco, G., Galvagno, S., and Parravano, G., *J. Catal.* **64**, 405 (1980).
18. Galvagno, S., Schwank, J., and Parravano, G., *J. Catal.* **61**, 223 (1980).
19. Taylor, K. C., *J. Catal.* **38**, 299 (1975).
20. Kubicka, H., *React. Kinet. Catal. Lett.* **5**, 223 (1976).
21. Kubicka, H., *J. Catal.* **12**, 233 (1968).
22. Goodwin, J. G., Jr., *J. Catal.* **68**, 227 (1981).
23. Dalla Betta, R. A., Piken, A. G., and Shelef, M., *J. Catal.* **35**, 54 (1974).
24. Sinfelt, J. H., and Yates, D. J. C., *J. Catal.* **8**, 82 (1967).
25. Dalla Betta, R. A., *J. Catal.* **34**, 57 (1974).
26. Vannice, M. A., *J. Catal.* **37**, 449 (1975).
27. Kemping, J. C., and Anderson, R. B., *Ind. Eng. Chem. Process Des. Dev.* **9**, 116 (1970).
28. Buyanova, N. E., Karnaukhov, A. P., Koroleva, N. G., Ratner, I. D., and Chernyavskaya, O. N., *Kinet. Katal.* **13**, 1364 (1972).
29. Speranskaya, G. V., Savel'eva, G. A., and Popova, N. M., *Kinet. Katal.* **22**, 407 (1972).
30. Schwank, J., Galvagno, S., and Parravano, G., *J. Catal.* **63**, 415 (1980).
31. Schuter, H., Terben, A., Gerhardt, W., *Z. Anorg. Allg. Chem.* **321**, 41 (1963).
32. Bell, W. E., and Tagami, M., *J. Phys. Chem.* **67**, 2432 (1963).
33. Kim, K. S., and Winograd, N., *J. Catal.* **35**, 66 (1974).
34. Sommerfeld, J. T., and Parravano, G., *J. Phys. Chem.* **69**, 102 (1965).
35. Schwank, J., *Gold Bull.* **16**, 103 (1983).
36. MacDonald, W. R., and Hayes, K. E., *J. Catal.* **18**, 115 (1970).
37. Fukushima, T., Galvagno, S., and Parravano, G., *J. Catal.* **57**, 177 (1979).
38. Shastri, A. G., Datye, A. K., and Schwank, J., *J. Catal.* **87**, 265 (1984).
39. Datye, A. K., and Schwank, J., *J. Catal.* **93**, 256 (1985).